Observation of resonances at subharmonics of the Rabi frequency in the saturated absorption of a 100% amplitude-modulated laser beam

Stephen Chakmakjian, Karl Koch, and C. R. Stroud, Jr.

The Institute of Optics, University of Rochester, Rochester, New York 14627

Received March 30, 1988; accepted May 26, 1988

A series of resonances has been observed in the absorption of a 100% amplitude-modulated laser beam by an optically pumped sodium atomic beam. Resonances were observed when the modulation frequency was equal to the first, second, and third subharmonic of the Rabi frequency. The experimental results are compared with theory, and the implications of these parametric resonances to laser instabilities are discussed.

INTRODUCTION

Researchers in the fields of modulation spectroscopy, optical bistability, and laser instability have become interested in the interaction of intense, strongly modulated fields with atomic systems.[1–7] A 100% amplitude-modulated (AM) field is a special case of strong modulation because the energy at the carrier frequency has been completely transferred into the modulation sidebands. In this paper we study the interaction of a 100% AM laser field with an ensemble of homogeneously broadened two-level atoms.

Under the influence of a strong resonant field the atomic variables undergo Rabi oscillations. If, in addition to the strong pump field, a weak probe field is applied, the probe field will see a complicated structure in its absorption spectrum owing to the presence of the strong field. When it is detuned from the strong field by the strong-field Rabi frequency, the probe field experiences a resonance in its absorption spectrum.[8–10] These results have been experimentally confirmed.[11–13] Sargent *et al.*[14] have shown how modulation techniques can be employed to probe the saturated absorption of these strongly driven atoms. Modulation techniques alleviate the need for a second laser. Instead, the strong field is weakly modulated at a tunable frequency, and the modulation sidebands probe the saturated absorption. Hillman *et al.*[15] and Kramer *et al.*[16] showed that the behavior seen in the absorption spectrum of the probe field is a result of the atomic response to the modulation tone in the field intensity. In their analysis they treated the interaction with the strong field to all orders, whereas the interaction with the sidebands was treated perturbatively. In the case of multiple strong fields it is necessary to treat all the field components and the combination tones to all orders.

Although the treatment of strong-modulation interactions is by no means complete, there has been experimental work in this area.[17–19] These strong-modulation experiments yield different results from those seen in weak-modulation experiments. The atomic variables exhibit resonant behavior when the modulation frequency is approximately equal to the Rabi frequency or any subharmonic of the Rabi frequency. Bonch-Bruevich *et al.*[17] performed an experiment with two strong rf fields tuned to a Zeeman resonance in cadmium. One rf field was held at a constant frequency while the other field was tuned about the resonance to obtain an absorption spectrum. The absorption spectrum of the rf fields exhibited several subharmonic resonances. Thomann[18] performed a three-field experiment at the sodium D_2 line resonance. The field was produced by strongly modulating a laser beam; the Rabi frequency was varied while the modulation frequency was held fixed. Although a center frequency (the carrier) was present in this experiment, the physics is similar to that in the two-field experiments. At this point it is helpful to review the theoretical predictions for the problem.[4,6,20–26]

THEORETICAL REVIEW

The response of an atomic system can be characterized, in part, by the rate at which it absorbs, or scatters, energy from a resonant laser beam. We employ a calculation developed by Hillman *et al.*[6] to calculate the rate of absorption from the optical Bloch equations

$$\dot{u} = -u/T_2 - \Delta v, \tag{1a}$$

$$\dot{v} = \Delta u - v/T_2 + \kappa E(t) w, \tag{1b}$$

$$\dot{w} = -(w+1)/T_1 - \kappa E(t) v, \tag{1c}$$

where Δ is the detuning and $1/T_2$ and $1/T_1$ are the polarization and population decay rates, respectively. The dipole coupling constant κ is given by

$$\kappa = 2d/\hbar, \tag{2}$$

where d is the dipole-moment matrix element and $\hbar$ is Planck's constant. We are interested in the response of an atom to a 100% AM excitation. In this case the electric field amplitude can be written as

$$E(t) = 2E_1 \cos(\delta\omega t), \tag{3}$$

where $\delta\omega$ is the modulation frequency and the amplitude of the electric field is E_1.

According to Floquet's theorem, the stationary-state re-

0740-3224/88/102015-06$02.00

sponse of the atomic variables can be expanded in a Fourier series of the modulation frequency $\delta\omega$. The atomic polarization components and the atomic inversion can be written as

$$u(t) = \sum_{n=-\infty}^{\infty} u_n \exp(in\delta\omega t), \tag{4a}$$

$$v(t) = \sum_{n=-\infty}^{\infty} v_n \exp(in\delta\omega t), \tag{4b}$$

and

$$w(t) = \sum_{n=-\infty}^{\infty} w_n \exp(in\delta\omega t). \tag{4c}$$

The nth-harmonic components of the in-phase and in-quadrature dipole moments and of the atomic inversion are denoted by u_n, v_n, and w_n, respectively. We substitute Eqs. (4) into the Bloch equations [Eqs. (1)] to obtain a set of recurrence relations between the harmonic components of the atomic variables. The ratio of the first-harmonic component of the in-quadrature dipole moment to the zeroth-harmonic (time-averaged) component of the inversion is expressed as a continued fraction:

$$\frac{v_1}{w_0} = \cfrac{1}{B_1 + \cfrac{I_1}{B_2 + \cfrac{I_1}{B_3 + \cfrac{I_1}{B_4 + \ldots}}}}, \tag{5}$$

where the single-field intensity is

$$I_1 = (\kappa E_1)^2 T_1 T_2 \tag{6}$$

and the coefficients denoted by B_n are

$$B_n = 1 + in\delta\omega T_2 + \frac{(\Delta T_2)^2}{1 + in\delta\omega T_2} \tag{7a}$$

for odd n and

$$B_n = 1 + in\delta\omega T_1 \tag{7b}$$

for even n. Note that the intensity is naturally expressed in dimensionless form in Eq. (6). We will use the dimensionless intensity as well as the dimensionless modulation frequency, $\delta\omega T_2$, and the dimensionless detuning, ΔT_2, throughout.

We can solve for the time-averaged component of the atomic inversion, w_0, in terms of the continued fraction and then write the excited-state population as

$$\rho_e = \frac{2I_1 \operatorname{Re}\{v_1/w_0\}}{1 + 2I_1 \operatorname{Re}\{v_1/w_0\}}. \tag{8}$$

We are ultimately interested in the absorption of the AM field. The average rate at which a two-level atom scatters light in the form of resonance fluorescence is proportional to the time-averaged absorption. The fluorescent emission rate is proportional to the excited-state population. Consequently, for the case of a 100% AM excitation of a two-level atom, the rate of absorption of energy is proportional to the time-averaged component of the excited-state population.

We plot the results of these calculations in Figs. 1 and 2. In Fig. 1 we plot the time-averaged excited-state population for a fixed Rabi frequency as a function of the modulation frequency, $\delta\omega T_2$. This curve is quite complicated, and it shows several resonances in the absorption spectrum of the fields. To understand these peaks it is helpful to solve the problem in the absence of damping. In this case we obtain an analytic solution in which the time-averaged response of the population can be written in terms of $J_0(2\kappa E_1/\delta\omega)$. When we numerically pick off the position of each peak from Fig. 1, we find that the peaks occur whenever the factor $J_0(2\kappa E_1/\delta\omega)$ is equal to zero. The outermost peaks correspond to the first zero of J_0. The next peaks, at smaller values of $\delta\omega T_2$, correspond to the second zero of J_0 and are the first subharmonic resonances. In the limit of large arguments, x, the zeros of $J_0(x)$ become equally spaced versus x. It is in this limit that the resonances are best described as

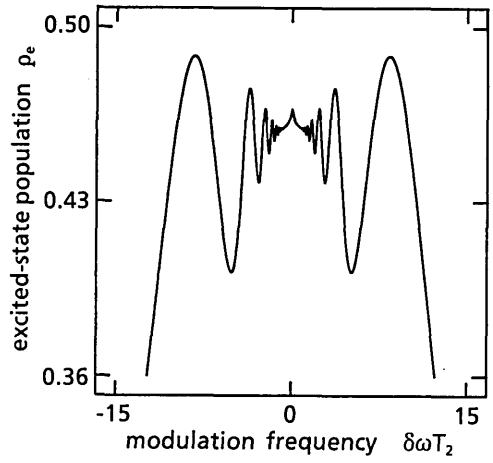

Fig. 1. Time-averaged excited-state population as a function of the modulation frequency $\delta\omega T_2$. The Rabi frequency is held fixed, $\kappa E_1 T_2 = 10$, and the modulation frequency $\delta\omega T_2$ is varied to observe the subharmonic resonances. The detuning is zero, $\Delta T_2 = 0$.

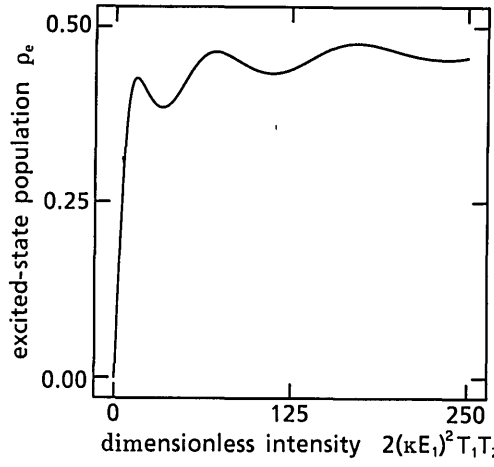

Fig. 2. Time-averaged excited-state population as a function of intensity. The modulation frequency is held fixed, $\delta\omega T_2 = 3$, and the time-averaged dimensionless intensity $2(\kappa E_1)^2 T_1 T_2$ is varied to observe the resonances. The detuning is zero, $\Delta T_2 = 0$.

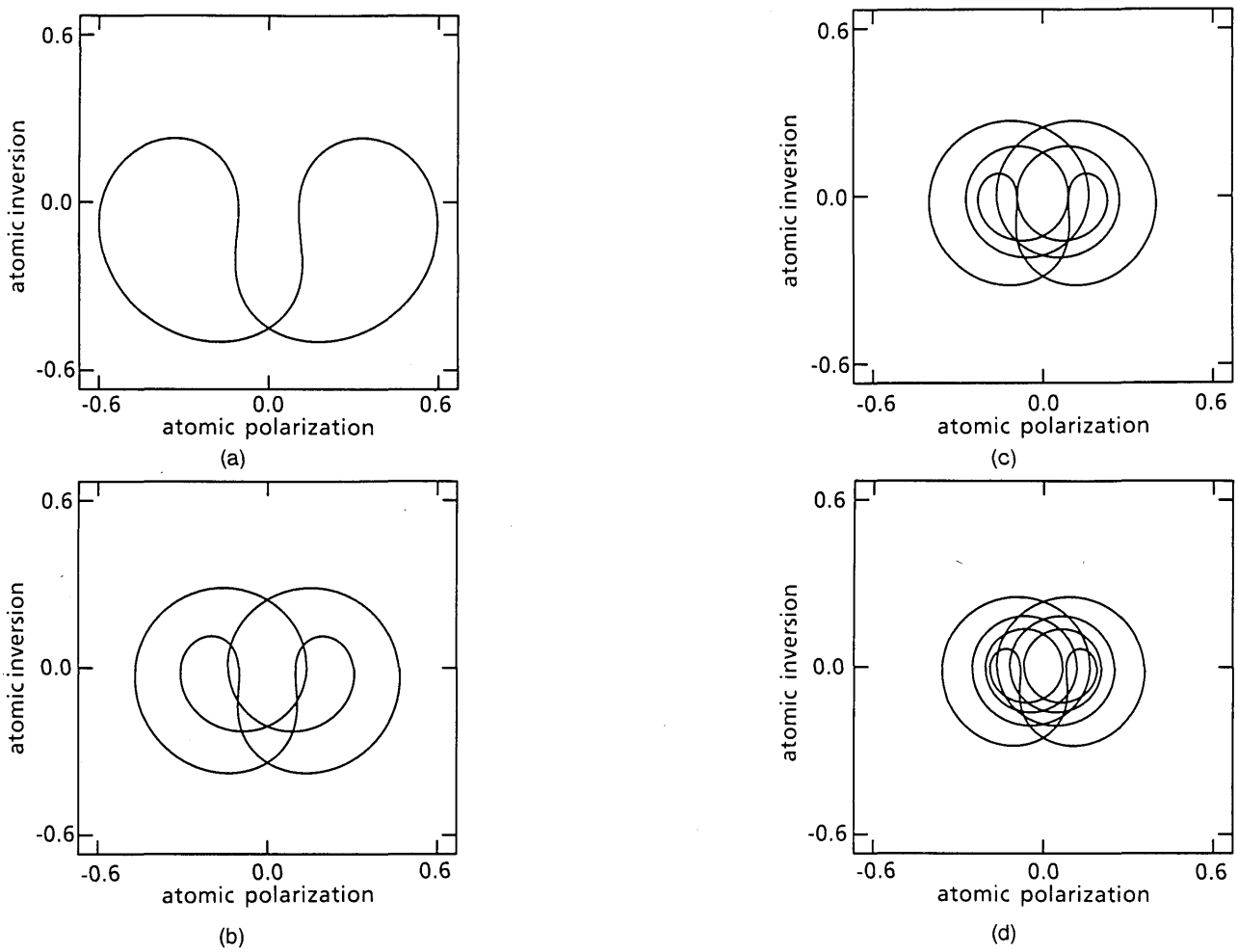

Fig. 3. Trajectories of the atomic inversion and the in-quadrature polarization. We plot the atomic inversion versus the atomic polarization at the first four resonances. The modulation frequency is $\delta\omega T_2 = 3$. In (a) the Rabi frequency corresponds to the first resonance. (b)–(d) Show the behavior at the first three subharmonic resonances: (b) $n = 2$, (c) $n = 3$, and (d) $n = 4$. The detuning is zero, $\Delta T_2 = 0$.

subharmonic resonances. In Fig. 2 the time-averaged population of the excited state is plotted versus the time-averaged dimensionless intensity $2(\kappa E_1)^2 T_1 T_2$ for a fixed modulation frequency of three atomic linewidths. This is the form of our raw data. The resonances appear as enhancements in the absorption embedded in the usual single-field saturation curve. As the intensity is increased from zero, we approach the first-order resonance. The second resonance, occurring at a higher intensity, is the first subharmonic resonance. The order of the subharmonic resonances increases as we look to higher dimensionless intensities. These resonances occur only when the modulation interaction is strong, meaning the Rabi frequency, κE_1, exceeds the natural linewidth of the transition and the modulation depth is large, as in the case of 100% amplitude modulation.

The dynamic behavior of the atomic variables also reflects the subharmonic behavior of the 100% AM interaction. In Figs. 3(a)–3(d), we show the phase plots formed by the in-quadrature atomic polarization and the inversion at each of the first four resonances (on-resonance excitation is used for the phase plots so that only the in-quadrature polarization is driven). Each section of Fig. 3 shows the trajectory followed by the atomic variables for a complete period of the modulation. Figure 3(a) shows the period-one behavior that occurs at the first resonance. Figure 3(b) shows that a second cycle in the trajectory occurs at the second resonance, which is the first subharmonic resonance. Figures 3(c) and 3(d) show the behavior at the third and fourth resonances, respectively. We can compare this system to an anharmonic oscillator being driven every nth cycle of its natural frequency. The oscillator can be driven effectively by the fundamental frequency or by any subharmonic of the fundamental. This subharmonic driving is effective because the system responds at higher harmonics of the driving frequency when the driving force is large enough to induce a nonlinearity.

EXPERIMENTAL SETUP

The experimental apparatus that we used to study the absorption spectrum is shown in Fig. 4. The absorption is determined by measuring the total fluorescence from a small portion of the interaction region. We imaged the fluorescence from the interaction region onto a pinhole placed in front of a photomultiplier tube. Spatially filtering the fluorescence signal limits the signal to that from a small region near the center of the laser beam, where the intensity is

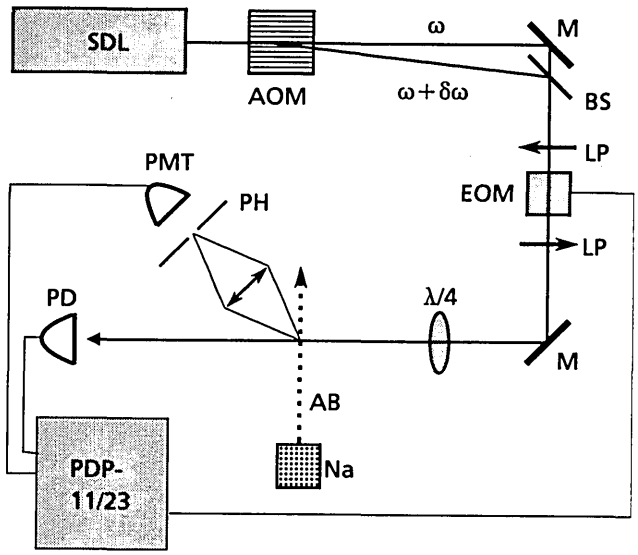

Fig. 4. Experimental apparatus: SDL, stabilized dye laser; AOM, acousto-optic modulator; M's, mirrors; BS, beam splitter; LP's, linear polarizers; EOM, electro-optic modulator; λ/4, quarter-wave plate; Na, sodium oven; AB, atomic beam; PH, pinhole; PMT, photomultiplier tube; PD, photodiode.

constant to within 10%. This allows us to study atoms with equal Rabi frequencies. The detectors were dc coupled to measure the time-averaged fluorescence.

Sodium was chosen as the atomic medium because it has a large oscillator strength and is readily made into a two-level atomic system. To obtain a two-level atomic system we resonantly excited the $3s$–$3p$ transition with circularly polarized light. A two-level system results from the pumping of the population into the aligned magnetic sublevels.[27] The atomic beam was collimated to provide a divergence angle of 1 mrad with an associated Doppler width of less than 2 MHz (this is 20% of the natural linewidth of the sodium transition). The atoms were excited by a circularly polarized beam whose angular divergence was less than 1 mrad (this angular spread accounts for no more than 1-MHz Doppler broadening). The laser field was the output of a frequency-stabilized Rhodamine 6G dye laser whose full-width frequency jitter was less than 1 MHz. The angular divergence of the laser and atomic beams, together with the frequency jitter of the laser, gave us a total systematic broadening of 4 MHz, or 40% of the natural linewidth. This systematic linewidth was verified by measuring the full spectral width of the atomic transition to be 14 MHz (the natural linewidth is 10 MHz).

We produced a 100% AM laser field with a modulation frequency, $\delta\omega/2\pi$, of 15 MHz, which is three times the polarization relaxation rate of the sodium D_2 line. The modulation was produced by passing the laser through a high-efficiency acousto-optic modulator. A portion of the beam was upshifted by the 30-MHz drive frequency of the acousto-optic modulator. The diffraction efficiency was adjusted so that the power diffracted into the first-order beam was equal to that remaining in the zeroth-order undiffracted beam. Then we recombined the two orders to create the bichromatic field. The two beams were aligned with interferometric precision so that a strong beat note of 30 MHz was clearly detected by a photodiode measuring the far-field intensity. After recombination the field state can be described in terms of a carrier, at the mean frequency of the two frequency components, that is 100% AM at one half the drive frequency of the acousto-optic modulator. Because the recombination geometry is different for each modulation frequency, it was inconvenient for us to vary the modulation frequency in search of the resonances. Instead, we held the modulation frequency fixed and varied the Rabi frequency by sweeping the intensity of the laser. This was done with a set of linear polarizers and an electro-optic cell driven by our computer.

At each power setting we recorded the incident laser intensity along with the intensity of the fluorescence emitted by the atoms. Each data point was averaged 100 times over several milliseconds to integrate out any fast intensity fluctuations of the laser field. All data were recorded with a 12-bit analog-to-digital converter on a PDP-11/23 microprocessor. The 36-dB dynamic range provided by the digitization is necessary to match the dynamic range of our data.

EXPERIMENTAL RESULTS

We collected data for the AM field on resonance and for a detuning of three linewidths. The modulation frequency was equal to three atomic linewidths for all the data that we present in this paper ($\delta\omega T_2 = 3$). In Fig. 5 we plot the fluorescent intensity versus the incident time-averaged intensity for on-resonance excitation. The resonances appear as bumps on the saturated absorption curve. The solid curve shows a theoretical fit to our data. A two-level theory is averaged over detuning and modulation frequency to model the slightly imperfect recombination of the two beams. When the two laser beams emerging from the acousto-optic modulator are not perfectly aligned (see Fig. 4), the atoms see a moving interference pattern. If this pattern moves along the atomic-beam axis, the spread in atomic velocities causes the atoms to experience a spread in modulation frequencies.

Because we are interested mainly in the resonances, we can divide our data by a single-frequency absorption curve to obtain a normalized atomic response to the two-field excitation. This normalization flattens out the curve so that the resonances may be seen on a single expanded graph. In Fig. 6 we plot the normalized fluorescent intensity versus the parameter $\sqrt{2}\kappa E_1 T_2$. The parameter $\sqrt{2}\kappa E_1$ is the rms Rabi frequency. A distinct enhancement in the absorption of the fields occurs when the rms Rabi frequency is equal to $n(2\delta\omega)$, where n is the number of the resonance and $2\delta\omega$ is the frequency difference between the two field modes. We can observe the first-order resonance and the first two subharmonic resonances with resonant excitation. With the fields detuned by three natural linewidths, we have observed up to three subharmonic resonances. In Fig. 7 we have plotted the fluorescent intensity versus the rms Rabi frequency for resonant and detuned excitation (for the detuned case $\Delta T_2 = 3$). The resonances occur at lower intensities when the modulated field is detuned because the generalized Rabi frequency is larger for the same amount of incident laser power. We do not have an analytical expression for the position of the resonance peaks. However, we find that the empirical formula

$$[(\sqrt{2}\kappa E_1)^2 + \Delta^2]^{1/2} = n(2\delta\omega) \tag{9}$$

describes the position of the resonances quite well for both detuned and resonant excitation. We can interpret the quantity of the left-hand side of Eq. (9) as the generalized Rabi frequency. A resonance occurs whenever the generalized Rabi frequency is equal to an integer, n, times the frequency separation, $2\delta\omega$, between the two fields. This formula for the resonances agrees with weak-modulation experiments.[11,13]

It is instructive to look at the positions of the resonances for the detuned and resonant modulated excitations. We used the computer to determine the position of the resonance peaks for the normalized data. The positions of these peaks for detuned and resonant excitation are plotted on the same graph in Fig. 8. The position of the nth resonance for the detuned case appears at a lower intensity than the corresponding resonance for the case of zero detuning. The solid line represents the theoretical predictions for the positions of the resonances according to Eq. (9).

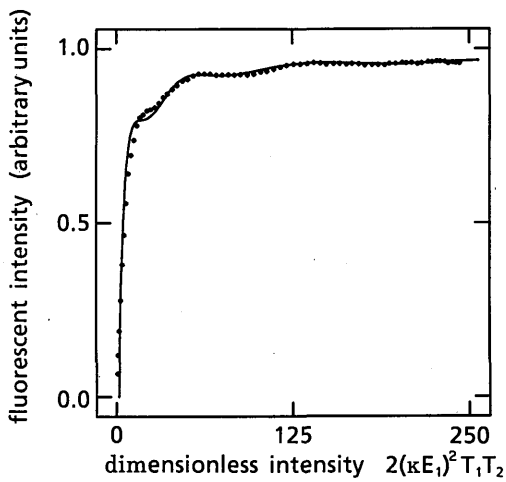

Fig. 5. Time-averaged fluorescent intensity versus time-averaged incident intensity. The raw data are plotted with dots, and the solid curve represents a best theoretical fit. The modulation frequency is fixed, $\delta\omega T_2 = 3$, and the detuning is zero, $\Delta T_2 = 0$.

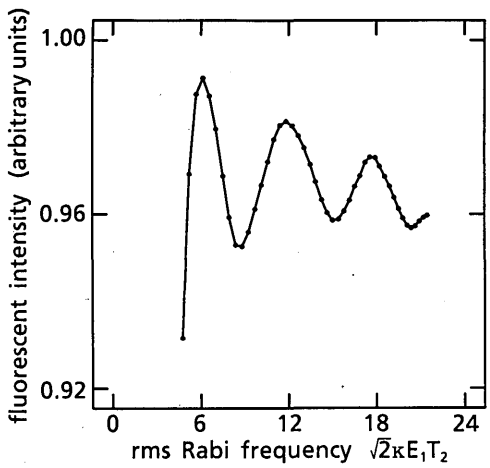

Fig. 6. Normalized time-averaged fluorescent intensity versus rms Rabi frequency for resonant excitation. The fluorescence data from Fig. 5 were normalized by a single-field saturation curve to flatten out the resonance peaks. The Rabi resonance and the first two subharmonic resonances are shown.

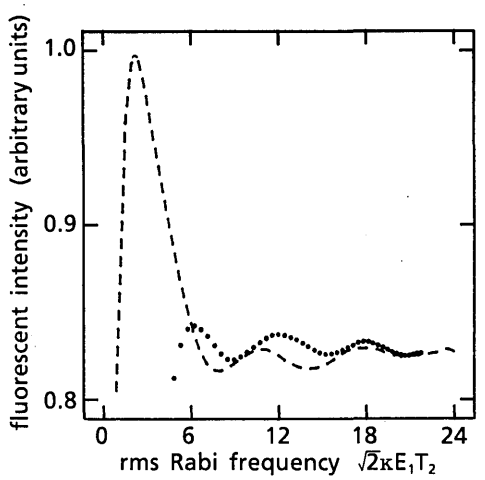

Fig. 7. Normalized time-averaged fluorescent intensity versus rms Rabi frequency for resonant and detuned excitation. The dotted curve represents the data for the resonant case, $\Delta T_2 = 0$. The dashed curve represents data for the detuned case, $\Delta T_2 = 3$. The resonant peaks occur at lower Rabi frequencies for the detuned case. The modulation frequency is $\delta\omega T_2 = 3$.

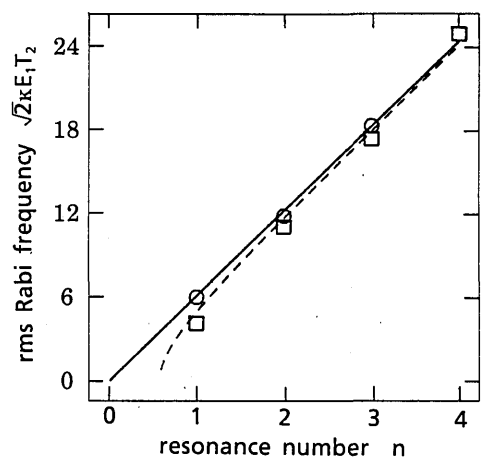

Fig. 8. The position of the subharmonic resonances versus resonance number for resonant and detuned excitation. The rms Rabi frequency, $\sqrt{2}\kappa E_1 T_2$, corresponding to the nth resonance is plotted versus n. The circles represent the data for resonant excitation, $\Delta T_2 = 0$. The squares represent the data for detuned excitation, $\Delta T_2 = 3$. The solid line represents the empirical expression in Eq. (9) for resonant excitation, $\Delta T_2 = 0$. The dashed curve represents Eq. (9) for $\Delta = \delta\omega$. The modulation frequency is $\delta\omega T_2 = 3$.

CONCLUSIONS

We have presented both theory and experiment for the absorption of a 100% AM field by a closed two-level atomic system. The interaction reveals resonances at subharmonics of the Rabi frequency. We observed the first three resonances with resonant excitation, and we observed the first four resonances with detuned excitation. For resonant excitation, the absorption of the AM field is enhanced whenever the ratio $2\kappa E_1/\delta\omega$ is equal to a zero of the zeroth-order Bessel function. In this paper we presented an empirical relation for the occurrence of the resonances for both resonant and detuned excitation. The data agree with this empirical prediction.

Our data show that the absorption of the bichromatic field is enhanced at the first-order resonance and at each of the

subharmonic resonances. This result differs from that obtained by Thomann.[18] The results of that experiment showed a decrease in the absorption at each resonance. In that experiment the field-modulation index was no larger than 0.65, so there was always a significant field component at the carrier frequency. When the carrier frequency is present, it can beat with each of the modulation sidebands to produce overtones, at harmonics of the modulation frequency, in the atomic response. This beat frequency is one half of the beat frequency arising between the two modulation sidebands. The harmonic overtones of these two sets of beat notes can destructively interfere in a three-field experiment. This interference causes the absorption to diminish at each resonance.

We have demonstrated the complicated behavior of a purely bichromatic field interacting with a closed, two-level atomic system. Subharmonic resonances occur because of the coherent nonlinear interaction of a multifrequency field with an isolated atomic resonance. It is exactly this type of nonlinear interaction that determines the competition or cooperation between cavity modes in a laser-gain medium. The same set of subharmonic resonances occurs in a saturated two-level amplifier interacting with a modulated laser field. This provides a mechanism for multimode instabilities in a homogeneously broadened laser. Instabilities of this type have been observed.[5]

ACKNOWLEDGMENTS

We wish to thank Lloyd W. Hillman for many useful conversations. We would also like to acknowledge support of this research by the U.S. Army Research Office.

REFERENCES

1. H. Risken and K. Nummedal, J. Appl. Phys. **39,** 4662–4672 (1968).
2. H. Risken and K. Nummedal, Phys. Lett. **26A,** 275–276 (1968).
3. B. J. Feldman and M. S. Feld, Phys. Rev. A **1,** 1375–1396 (1970).
4. N. Tsukada and T. Nakayama, Phys. Rev. A **25,** 964–977 (1982).
5. L. W. Hillman, J. Krasinski, R. W. Boyd, and C. R. Stroud, Jr., Phys. Rev. Lett. **52,** 1605–1608 (1984).
6. L. W. Hillman, J. Krasinski, K. Koch, and C. R. Stroud, Jr., J. Opt. Soc. Am. B **2,** 211–217 (1985).
7. T. Ogawa and E. Hanamura, Appl. Phys. B **43,** 139–153 (1987).
8. B. R. Mollow, Phys. Rev. A **5,** 2217–2222 (1972).
9. R. Saxena and G. S. Agarwal, J. Phys. B **12,** 1939–1951 (1979).
10. R. W. Boyd, M. G. Raymer, P. Narum, and D. J. Harter, Phys. Rev. A **24,** 411–423, (1981).
11. F. Y. Wu, S. Ezekiel, M. Ducloy, and B. R. Mollow, Phys. Rev. Lett. **38,** 1077–1080 (1977).
12. D. J. Harter, P. Narum, M. G. Raymer, and R. W. Boyd, Phys. Rev. Lett. **46,** 1192–1195 (1981).
13. M. T. Gruneisen, K. R. MacDonald, and R. W. Boyd, J. Opt. Soc. Am. B **5,** 123–129 (1988).
14. M. Sargent III, P E. Toschek, and H. G. Danielmeyer, Appl. Phys. **11,** 55–62 (1976).
15. L. W. Hillman, R. W. Boyd, and C. R. Stroud, Jr., Opt. Lett. **7,** 426–428 (1982).
16. M. A. Kramer, R. W. Boyd, L. W. Hillman, and C. R. Stroud, Jr., J. Opt. Soc. Am. B **2,** 1444–1455 (1985).
17. A. M. Bonch-Bruevich, T. A. Vartanyan, and N. A. Chigir, Sov. Phys. JETP **50,** 901–906 (1979).
18. P. Thomann, J. Phys. B **13,** 1111–1124 (1980).
19. R. E. Silverans, G. Borghs, P. De Bisschop, and M. Van Hove, Phys. Rev. Lett. **55,** 1070–1073 (1985).
20. P. Thomann, J. Phys. B. **9,** 2411–2419 (1976).
21. G. I. Toptygina and E. E. Fradkin, Sov. Phys. JETP **55,** 246–251 (1982).
22. An. A. Mak, S. G. Przhibel'skii, and N. A. Chigir, Ser. Fiz. **47,** 1976–1983 (1983).
23. G. S. Agarwal and N. Nayak, J. Opt. Soc. Am. B **1,** 164–168 (1984).
24. W. M. Ruyten, L. M. Davis, C. Parigger, and D. R. Keefer, *Advances in Laser Science-III*, A. C. Tam, J. L. Gole, and W. C. Stwalley, eds. (American Institute of Physics, New York, 1988).
25. J. H. Eberly and V. D. Popov, Phys. Rev. A **37,** 2012–2016 (1988).
26. T. W. Mossberg and M. L. Lewenstein, Department of Physics, University of Oregon, Eugene, Oregon 97403 (personal communication).
27. J. A. Abate, Opt. Commun. **10,** 269–272 (1974).